Materials Science in Semiconductor Processing 27 (2014) 494–499

Contents lists available at ScienceDirect

Materials Science in Semiconductor Processing

journal homepage: www.elsevier.com/locate/mssp

Synthesis of pristine In_2O_3/ZnO–In_2O_3 composited nanotubes and investigate the enhancement of their acetone sensing properties

Xiao Chi [a], Changbai Liu [b], Yu Li [a], Haiying Li [a], Li Liu [a,*], Xiaoqing Bo [a], Lili Liu [a], Chang Su [a]

[a] State Key Laboratory of Superhard Materials, College of Physics, Jilin University, Changchun 130012, PR China
[b] College of Electronic Science & Engineering, Jilin University, Changchun 130012, PR China

ARTICLE INFO

Available online 8 August 2014

Keywords:
In_2O_3
Nanotubes
ZnO
Gas sensor
Acetone

ABSTRACT

Pristine In_2O_3 and ZnO–In_2O_3 composited nanotubes were synthesized by the electrospinning technic and followed by calcination. The formation of ZnO–In_2O_3 n–n heterojunctions was found to be highly sensitive to acetone gas. X-ray powder diffraction (XRD), Scanning electron microscope (SEM) and energy dispersive X-ray spectrometry (EDS) were respectively used to characterize surface crystallinity and morphology. The possible mechanism of nanotubes formation was also investigated. Gas sensors were made based on the as-synthesized materials to investigate their gas sensing properties. Compare with the pristine In_2O_3 nanotubes, ZnO–In_2O_3 composite nanotubes show the obviously improved of acetone sensitivity. The sensitivity of ZnO–In_2O_3 composite nanotubes is about 43.2, which is about triple times larger than that of the pristine In_2O_3 nanotubes to 60 ppm acetone at 280 °C. The response and recovery times of ZnO–In_2O_3 nanotubes to 60 ppm acetone are about 5 and 25 s. In addition, ZnO–In_2O_3 composite nanotubes sensor also possesses a good selectivity to acetone.

1. Introduction

Recent years, chemical sensors for acetone (CH_3COCH_3) detection have attracted lots of attentions for the increasing concern about industrial pollution, environmental protection and human health [1,2]. So far, lots of efforts have been made to develop efficient detectors. As one of the most widely studied metal oxide semiconductors, In_2O_3 have been proved to be a candidate for sensors application. There are many kinds of gases have been recognized by In_2O_3 sensors, such as acetone, ethanol, formaldehyde, nitrogen dioxide, hydrogen, carbon monoxide and et al. [3–8]. ZnO is also a kind of important metal oxide semiconductor and attracts lots of interests for its gas sensing properties [9–11]. Therein, some ZnO acetone sensors have been investigated for its acetone sensing properties [12,13].

Doping metal or metal oxides, adding catalysts, downsizing semiconductor, morphology controlling and forming pore are all have significant effect upon the performance of the gas sensing property. Taking the advantages of open morphology and small size, many types of sensors based on In_2O_3 or ZnO nanostructures have been made [14,15]. One-dimensional nanostructure about gas sensing property has been studied a lot because it can improve the

* Corresponding author at: College of Physics, Jilin University, 2699 Qianjin Street, Changchun, Jilin Province 130012, PR China.
Tel./fax: +86 431 88502260.
E-mail address: liul99@jlu.edu.cn (L. Liu).

http://dx.doi.org/10.1016/j.mssp.2014.07.032
1369-8001/

efficiency of translating the gas recognition into electrical signal and the transport electron [16]. In order to enhance the gas sensing property, adding some certain amount other kind of metal or mental oxide is also efficiency.

Electrospinning is an efficient method to synthesize one-dimensional nanostructure materials. In this work, pristine In_2O_3 and ZnO–In_2O_3 composited nanotubes were fabricated by electrospinning and followed by annealing. Acetone sensing property of the sensor was investigated based on ZnO–In_2O_3 composite nanotubes. The results reveal that ZnO–In_2O_3 composited nanotubes show the improved sensitivity to acetone. Moreover, compare with pristine In_2O_3 nanotubes, ZnO–In_2O_3 composite nanotubes show a significant enhancement for acetone sensitivity.

2. Experiment

2.1. Chemicals

Indium nitrate hydrate ($In(NO_3)_3$, 99.99%), zinc nitrate ($Zn(NO_3)_2 \cdot 6H_2O$, 99.99%), ethanol ($\geq$ 99.5%) and *N*,*N*-dimethylformamide (DMF, $\geq$ 99.9%) were purchased from Aladdin (China). Polyvinyl pyrrolidone (PVP, Mw = 1300,000) was purchased from Sigma-Aldrich (America). All of chemicals were used without any further purification.

2.2. Preparation of pristine In_2O_3 and ZnO–In_2O_3 composited nanotubes

The pristine In_2O_3 and ZnO–In_2O_3 composited nanotubes were synthesized by electrospinning and followed by annealing. The composited nanotubes were synthesized as follows. In a typical procedure, 0.4 g $In(NO_3)_3$ and 0.0074 g $Zn(NO_3)_3 \cdot 6H_2O$ were mixed with 5 g DMF, via the magnetic stirring for 30 min. Then, 1.5 g PVP, 14 g ethanol was added into the above solution and stirred for 30 min. The mixed solution was kept stirring for 10 h and the precursor solution was obtained. Subsequently, the precursor was loaded into a syringe and supplied the high voltage. During the electrospinning process, the distance between the anode (the syringe) and cathode (the flat foil) is 20 cm and 15 kV was supplied. Finally, the composite nanofibers were collected and annealed at 550 °C for 3 h with a heating rate of 10 °C/min. The pristine In_2O_3 nanotubes were prepared under the same process without added $Zn(NO_3)_3 \cdot 6H_2O$.

2.3. Sensor fabrication

The as-synthesized ZnO–In_2O_3 composited nanotubes were mixed with deionized water and formed a paste. The paste was coated on the ceramic tube that a pair of gold electrodes was previously printed. Then, a Ni-Cr heating wire was inserted into the tube as a heater for sensor. The gas sensor was dried and aged for about 3 days before the first measurement. Gas sensing experiments were tested by CGS-8 intelligent gas sensing analysis system (Beijing Elite Tech Co., Ltd., China).

The sensor response (S) is defined as $S = R_a/R_g$. R_a is the resistance of sensor in the ambient air and R_g is the resistance of sensor in the target gas. The response and recovery times are defined by the time spend on the sensor to achieve 90% of the total resistance change in the case of adsorption and desorption, respectively.

2.4. Characterization and measurement

The images of nanotubes were characterized by Scanning electron microscope (SEM, FEI, XL30ESEM) instrument. X-ray powder diffraction (XRD, Rigaku, Ultima IV) instrument were used to characterize the structure of nanotubes with Cu $K\alpha 1$ radiation ($\lambda = 1.5406$ Å). Energy dispersive X-ray spectrometry (EDS) was performed using an FEI XL30ESEM-FEG system.

3. Results and discussion

3.1. Morphological and structural characteristics

The structures and morphologies of the In_2O_3 and ZnO–In_2O_3 samples were characterized by SEM and the results are shown in Fig. 1. The pristine In_2O_3 nanotubes SEM images are shown in Fig. 1(a and b). Fig. 1(c and d) show the SEM images of ZnO–In_2O_3 composited nanotubes. From the SEM images it is clear to see that the morphology of these images is nanotubes. The average diameter of nanotubes is about 300 nm. The morphology of nanotubes can enhance the gas absorption.

In our opinions, the heating rate and the proportion of precursor solution are both have importance effects on the formation of In_2O_3 nanotubes. During the electrospinning course, the nanofibers were first synthesized which consist of PVP, ethanol, DMF and $In(NO_3)_3$. When the as-synthesized nanofibers were annealed in furnace, the surface of nanofibers was first oxidated for the heating rate was so fast and leaded to the unbalance of nanofibers inside and outside. Ethanol, DMF and PVP were decomposed for annealing. With the temperature increasing, the inside $In(NO_3)_3$ was also oxidated and adhere to the previously oxidated $In(NO_3)_3$ outside. During the above nanotubes formation process, the low ratio of $In(NO_3)_3$/PVP was also play a very importance role of nanotubes formation. For the low amount of $In(NO_3)_3$ in as-synthesized nanofibers, the inside oxidated In_2O_3 have to adhere to the outside firstly oxidated In_2O_3 for the strain strength. Finally, the In_2O_3 nanotubes were synthesized after the annealing process. The ZnO–In_2O_3 composited nanotubes were also synthesized for the above nanotubes forming mechanism.

The XRD patterns of pristine In_2O_3 and ZnO–In_2O_3 composited nanotubes are shown in Fig. 2. Each strong diffraction peak in Fig. 2 can be indexed as the cubic structure of In_2O_3 (JCPDS card 71-2194). There is no obvious zinc or zinc compounds peak can be observed from the XRD pattern. This phenomenon can be ascribe to the amount of ZnO is too low for detection. Compared with the diffraction peaks of ZnO–In_2O_3 composited nanotubes, the pristine In_2O_3 diffraction peaks are more sharp and strong. This phenomenon can be ascribed to the radius of In^{3+} (0.80 Å) is bigger than that Zn^{2+} (0.74 Å) [17,18]. For doping where Zn^{2+} may replace the In^{3+} site and make

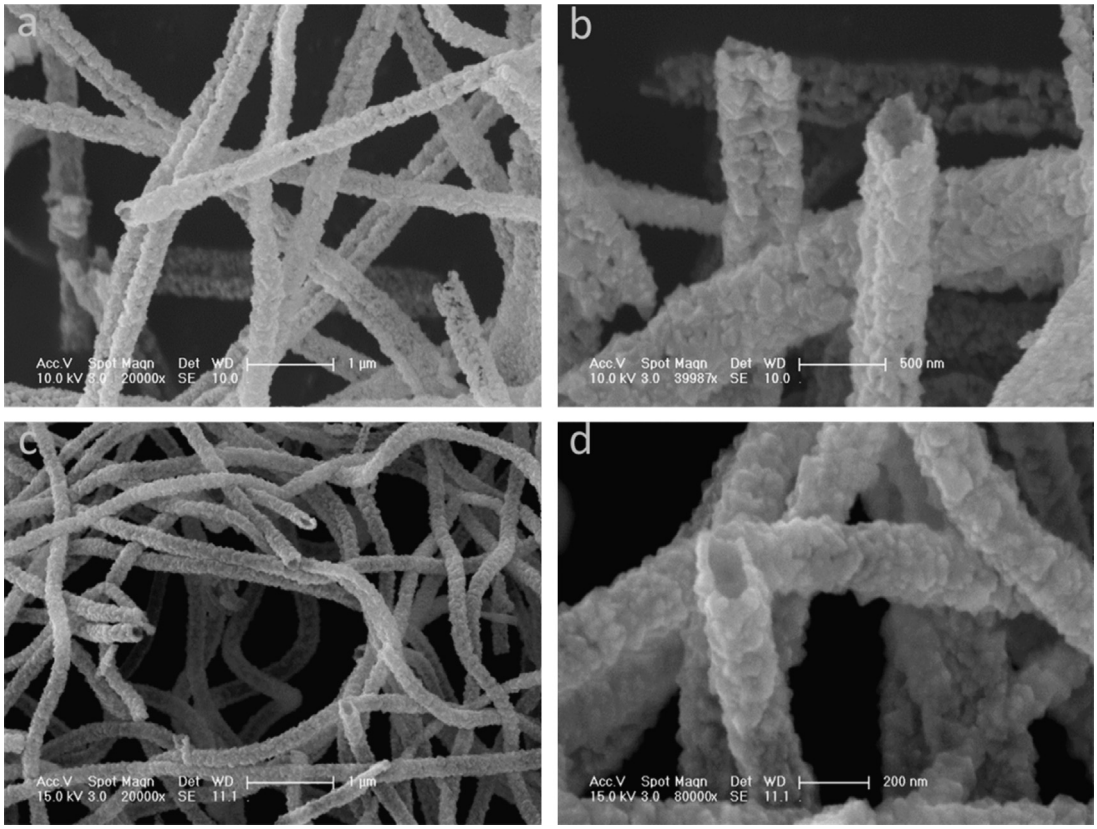

Fig. 1. SEM images of ((a) and (b)) pristine In_2O_3 nanotubes and ((c) and (d)) ZnO–In_2O_3 composited nanotubes.

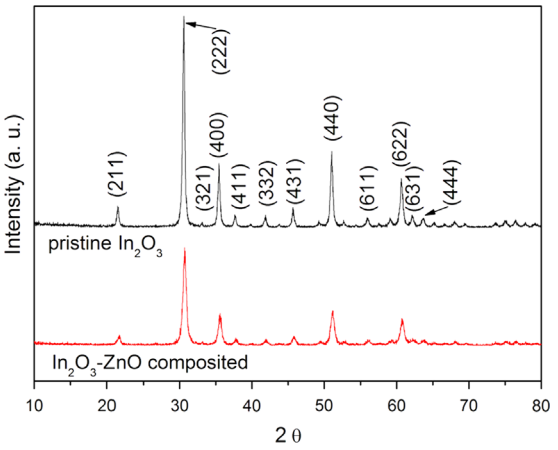

Fig. 2. XRD patterns of pristine In_2O_3 and ZnO–In_2O_3 composited nanotubes.

the grain shrink. As a result, the grain size is smaller for the ZnO adding. According to the Scherrer formular [19,20],

$$D = K\lambda/\beta \cos(\theta) \quad (1)$$

where D is the grain size, K is 0.89, λ is the wavelength of X-ray radiation ($\lambda = 0.15406$ nm), β is the full width at half-maximum of diffraction peak at 2θ. Wide diffraction peak means a high β and a small grain size. In order to further verify the above conjecture, we choose the highest peak (2 2 2) for each XRD pattern. The grain sizes of pristine In_2O_3 and ZnO–In_2O_3 composited nanotubes were calculated to be 24.20 and 19.47 nm which further confirmed the above conjecture.

Fig. 3 shows the EDS data for ZnO–In_2O_3 nanotubes which reveal the presence of Zn, which further indicates that the samples are composed of In, Zn, C and O elements. The samples were capped with Pt before EDS test. C element may come from the incomplete decomposition of PVP.

3.2. Gas sensing properties

In order to find the optimum working temperature of our samples, gas sensing experiments were firstly operated at different temperatures. Fig. 4 shows the responses of pristine In_2O_3 and ZnO–In_2O_3 composite nanotubes sensors to 60 ppm acetone at different operating temperature. From this Fig. 4 we can find that each curve increases and reaches its highest response at 280 °C, and then decreases rapidly with the increasing temperature. This phenomenon can be attributed to the balance between the formation of O^- ions (formation rate is increased with the temperature increase) and the adsorptive reaction (reaction rate is decreased with the temperature increase) [21]. The formation of various sorts of oxygen ions formula is as

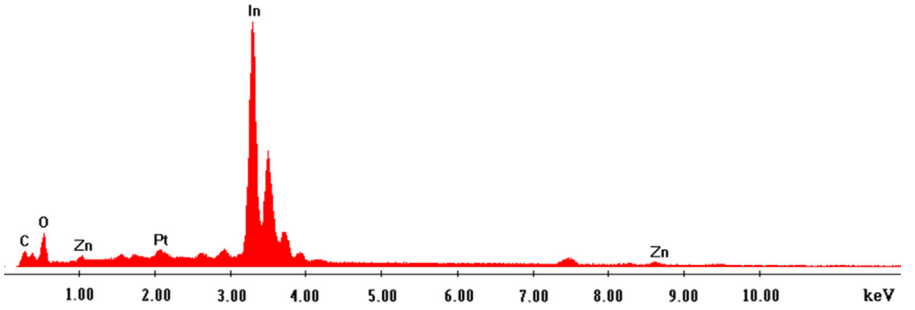

Fig. 3. EDS pattern of ZnO–In_2O_3 compose nanotubes.

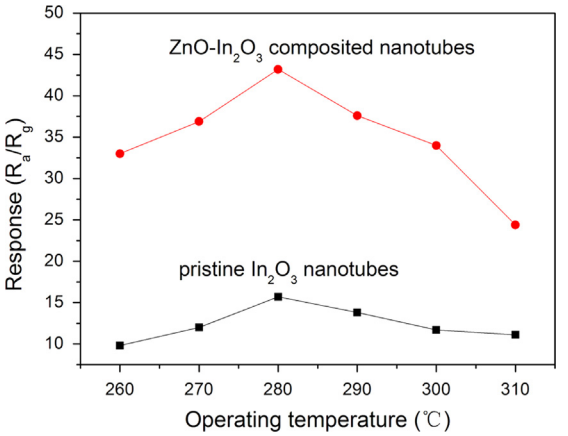

Fig. 4. Responses of pristine In_2O_3 and ZnO–In_2O_3 composited nanotubes sensors to 60 ppm acetone at different operating temperature.

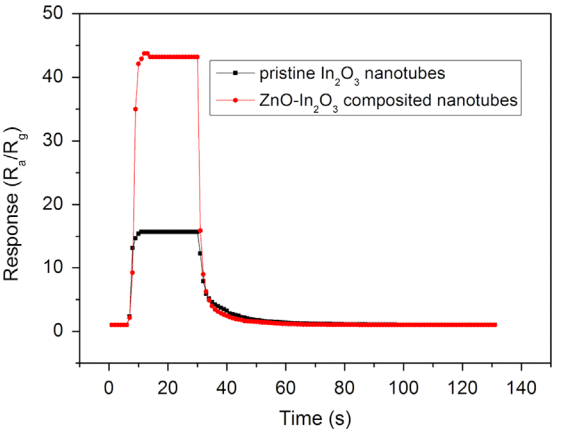

Fig. 5. Response and recovery curves of sensors based on the pristine In_2O_3, and ZnO–In_2O_3 composited nanotubes to 60 ppm acetone at 280 °C.

follows.

$$O_{2(gas)} \rightarrow O_{2\ (ads)} \tag{2}$$

$$O_{2\ (ads)} + e^- \rightarrow O^-_{2\ (ads)} (T \leq 100\ ^\circ C) \tag{3}$$

$$O^-_{2\ (ads)} + e^- \rightarrow 2O^-_{(ads)} (100 < T < 300\ ^\circ C) \tag{4}$$

Compared with the pristine In_2O_3 nanotubes, ZnO–In_2O_3 composite nanotubes sensor has a better sensitivity and the response is about 43.2. 280 °C was chosen as the working temperature.

The real time response and recovery characteristic plays an important role in analyzing the gas sensing properties for gas sensor. Fig. 5 shows the real time response and recovery characteristics based on the pristine In_2O_3 and ZnO–In_2O_3 composite nanotubes sensor to 60 ppm acetone at 280 °C. From Fig. 5 we can see when the sensors were exposed in the target gas circumstance, the response rapidly increased and got a stable value. Then, when the gas sensor was exposed in the air, the response value gradually decreased and recovered back to the original value in air. The response and recovery times changes slightly and this phenomenon can be ascribed to the slightly composited ZnO have little effect on response and recovery times. The response times of sensors are about 5 s based on each sensor. The recovery times are approximately 25 s. The composited nanotubes sensor has better response can be ascribe to the formation of heterojunction between ZnO and In_2O_3 [22]. ZnO and In_2O_3 are both n-type semiconductors. ZnO possesses a lower band gap (E_g=3.37 eV) than that of In_2O_3 (E_g=3.75 eV). At the interface of ZnO–In_2O_3, the electrons will transport from In_2O_3 to ZnO. As a result, slight ZnO will accumulate more electrons. At the interface, accumulation layer will be formed next to the ZnO and depletion layer will be formed next to the In_2O_3. When the ZnO–In_2O_3 composited nanotubes sensor exposed to target gas, heterojunction can provide much more electron for reaction and lead a better response.

In order to further express the sensitivity of the ZnO–In_2O_3 composited nanotubes, sensor was exposed to different concentration acetone at 280 °C and the responses are shown in Fig. 6. In Fig. 6b, the results indicate that the lowest detectable concentration of acetone is about 0.125 ppm, which possesses the value of 2.04. It is an excellent and acceptable response value. Fig. 6 shows that the response curve increases rapidly at the beginning (< 10,000 ppm). With the acetone concentration increased, the response slowly increased and gradually saturated. When the sensor exposed to 25,000 ppm acetone, the response increased little and saturated. It is can be explained that there is no more O^- ions on the nanotubes surface react with acetone molecules when the corresponding sensor was exposed in acetone [23].

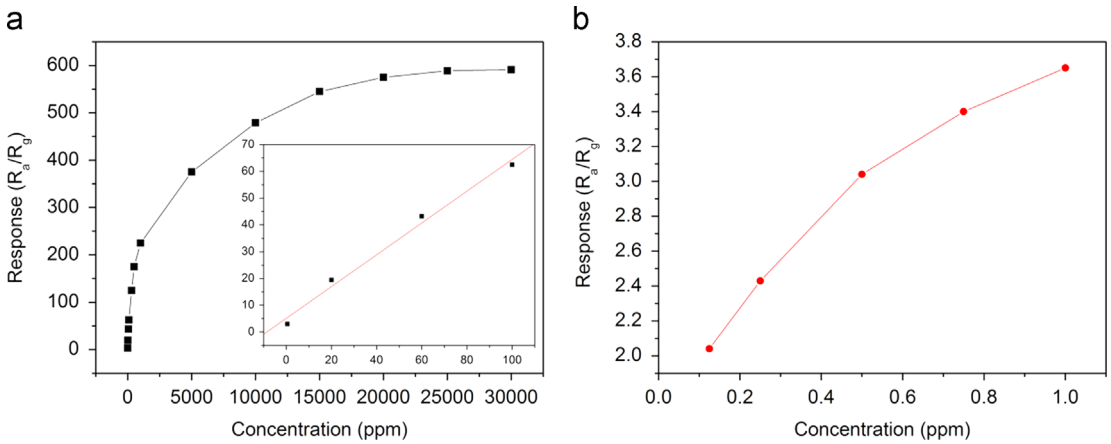

Fig. 6. (a) The saturated response curve of ZnO–In_2O_3 composited nanotubes to different concentration acetone at 280 °C, the insert show the response from 0.5 to 100 ppm acetone. (b) The response curve of ZnO–In_2O_3 composited nanotubes to acetone from 0.125 to 1 ppm at 280 °C.

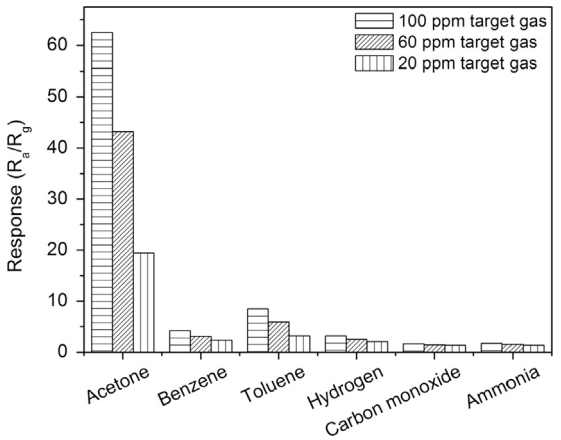

Fig. 7. Responses of ZnO–In_2O_3 composited nanotubes sensor to 20, 60 and 100 ppm acetone, benzene, toluene, hydrogen, carbon monoxide and ammonia at 280 °C.

In our further experiments, acetone, benzene, toluene, hydrogen, carbon monoxide and ammonia were chosen to test their gas sensing properties under the same condition based on ZnO–In_2O_3 composited nanotubes sensor. Fig. 7 shows the sensitivities of ZnO–In_2O_3 composited nanotubes sensor to 20, 60 and 100 ppm, respectively. We can observe that the composited nanotubes sensor possesses a far higher response than that of benzene, toluene, hydrogen, carbon monoxide and ammonia. Different kinds of gases have different responses under the same condition can be attributed to different gases possess different inherent energies level for adsorption, desorption and reaction with active sites on the surface of the sensing materials [24].

4. Conclusions

In summary, pristine In_2O_3 nanotubes and ZnO–In_2O_3 composited nanotubes were prepared by the method of electrospinning and followed by annealing. The results of the experiments reveal that ZnO–In_2O_3 composited can immensely enhance acetone sensing properties based on In_2O_3 nanotubes. The response of ZnO–In_2O_3 composited nanotubes gas sensor to 60 ppm acetone is about 43.2, which is almost 3 times larger than that of the pristine In_2O_3 nanotubes. The response and recovery times are about 5 and 25 s, respectively. The lowest detection is 0.125 ppm, which possesses an acceptable value of 2.04. Moreover, the corresponding gas sensor also has good selectivity to benzene, toluene, hydrogen, carbon monoxide and ammonia. These results reveal that ZnO–In_2O_3 composited nanotubes gas sensors may become a good candidate for practical application of acetone sensor.

Acknowledgements

The work has been supported by the National Innovation Experiment Program for University Students (2010C65188), and the Jilin Provincial Science and Technology Department (20140204027GX).

References

[1] M. Bettoni, P. Candori, S. Falcinelli, F. Marmottini, S. Meniconi, C. Rol, G.V. Sebastiani, J. Photochem. Photobiol., A 268 (2013) 1–6.
[2] Y. Zhang, W. He, H. Zhao, P. Li, Vacuum 95 (2013) 30–34.
[3] H. Dong, Y. Liu, G. Li, X. Wang, D. Xu, Z. Chen, T. Zhang, J. Wang, L. Zhang, Sens. Actuators, B 178 (2013) 302–309.
[4] S. An, S. Park, H. Ko, C. Jin, W.I. Lee, C. Lee, J. Phys. Chem. Solids 74 (7) (2013) 979–984.
[5] P. Song, Q. Wang, Z. Yang, Sens. Actuators, B 168 (2012) 421–428.
[6] M.W.K. Nomani, D. Kersey, J. James, D. Diwan, T. Vogt, R.A. Webb, G. Koley, Sens. Actuators, B 160 (1) (2011) 251–259.
[7] B.-R. Huang, J.-C. Lin, Sens. Actuators, B 174 (2012) 389–393.
[8] N. Singh, R.K. Gupta, P.S. Lee, ACS Appl. Mater. Interfaces 3 (7) (2011) 2246–2252.
[9] B.-Y. Wang, D.-S. Lim, Y.-J. Oh, CO Gas, Jpn. J. Appl. Phys. 52 (2013) 101103.
[10] N.S. Ramgir, M. Kaur, P.K. Sharma, N. Datta, S. Kailasaganapathi, S. Bhattacharya, A.K. Debnath, D.K. Aswal, S.K. Gupta, Sens. Actuators, B 187 (2013) 313–318.
[11] Ö. Çoban, S. Tekmen, S. Tüzemen, Sens. Actuators, B 186 (2013) 781–788.
[12] H. Song, H. Yang, X. Ma, J. Alloys Compd 578 (2013) 272–278.
[13] X. Yu, F. Song, B. Zhai, C. Zheng, Y. Wang, Physica E 52 (2013) 92–96.
[14] S. Cho, D.-H. Kim, B.-S. Lee, J. Jung, W.-R. Yu, S.-H. Hong, S. Lee, Sens. Actuators, B 162 (1) (2012) 300–306.
[15] S.-J. Kim, I.-S. Hwang, J.-K. Choi, Y.C. Kang, J.-H. Lee, Sens. Actuators, B 155 (2) (2011) 512–518.

[16] Z. Wang, Z. Li, L. Liu, X. Xu, H. Zhang, W. Wang, W. Zheng, C. Wang, A Novel, J. Am. Ceram. Soc. 93 (3) (2010) 634–637.
[17] H. Baqiah, N.B. Ibrahim, M.H. Abdi, S.A. Halim, J. Alloys Compd 575 (2013) 198–206.
[18] Y. Wang, F. Luo, L. Zhang, D. Zhu, W. Zhou, Ceram. Int. 39 (8) (2013) 8723–8727.
[19] P. Praveen, G. Viruthagiri, S. Mugundan, N. Shanmugam, Spectrochim. Acta, Part A 117 (2014) 622–629.
[20] M.H. Kim, Y. Chan Kang, S.M. Jeong, Y.J. Choi, Y.S. Kim, Mater. Chem. Phys. 142 (1) (2013) 438–444.
[21] S.K. Lim, S.-H. Hwang, D. Chang, S. Kim, Sens. Actuators, B 149 (1) (2010) 28–33.
[22] P. Li, H. Fan, Y. Cai, Sens. Actuators, B 185 (2013) 110–116.
[23] Z. Wang, Z. Li, J. Sun, H. Zhang, W. Wang, W. Zheng, C. Wang, J. Phys. Chem. C 114 (13) (2010) 6100–6105.
[24] S.T. Navale, D.K. Bandgar, S.R. Nalage, G.D. Khuspe, M.A. Chougule, Y.D. Kolekar, S. Sen, V.B. Patil, Ceram. Int. 39 (6) (2013) 6453–6460.